



Polymer photonic crystal dye lasers as optofluidic cell sensors

Christiansen, Mads Brøkner; Lopacinska, Joanna M.; Jakobsen, Mogens Havsteen; Mortensen, Niels Asger; Dufva, Hans Martin; Kristensen, Anders

Published in:
Optics Express

Link to article, DOI:
[10.1364/OE.17.002722](https://doi.org/10.1364/OE.17.002722)

Publication date:
2009

Document Version
Publisher's PDF, also known as Version of record

[Link back to DTU Orbit](#)

Citation (APA):
Christiansen, M. B., Lopacinska, J. M., Jakobsen, M. H., Mortensen, N. A., Dufva, H. M., & Kristensen, A. (2009). Polymer photonic crystal dye lasers as optofluidic cell sensors. *Optics Express*, 17(4), 2722-2730. <https://doi.org/10.1364/OE.17.002722>

General rights

Copyright and moral rights for the publications made accessible in the public portal are retained by the authors and/or other copyright owners and it is a condition of accessing publications that users recognise and abide by the legal requirements associated with these rights.

- Users may download and print one copy of any publication from the public portal for the purpose of private study or research.
- You may not further distribute the material or use it for any profit-making activity or commercial gain
- You may freely distribute the URL identifying the publication in the public portal

If you believe that this document breaches copyright please contact us providing details, and we will remove access to the work immediately and investigate your claim.

Polymer photonic crystal dye lasers as Optofluidic Cell Sensors

Mads Brøkner Christiansen¹, Joanna Malgorzata Lopacinska¹,
Mogens Havsteen Jakobsen¹, Niels Asger Mortensen², Martin Dufva¹
and Anders Kristensen¹

¹Department of Micro and Nanotechnology, DTU Nanotech

²Department of Photonics Engineering, DTU Fotonik

Technical University of Denmark

DK-2800 Kongens Lyngby, Denmark

anders.kristensen@nanotech.dtu.dk

<http://www.nanotech.dtu.dk/ak>

Abstract: Dye doped hybrid polymer lasers are implemented as label free evanescent field biosensors for detection of cells. It is demonstrated that although the coverage is irregular and the cells extend over several lattice constants, the emission wavelength depends linearly on the fraction of the surface covered by the HeLa cells used as model system. Design parameters relating to photonic crystal sensing of large objects are identified and discussed. The lasers are chemically modified to bind cells and molecules with flexible UV activated linker molecules.

© 2009 Optical Society of America

OCIS codes: (140.2050) Dye Lasers; (050.5298) Photonic crystals; (280.1415) Biological sensing and sensors

References and links

1. X. Fan, I. M. White, S. I. Shopoua, H. Zhu, J. D. Suter, and Y. Sun, "Sensitive optical biosensors for unlabeled targets: A review," *Anal. Chim. Acta* **620**, 8–26 (2008).
2. D. Erickson, C. Yang, and D. Psaltis, "Optofluidics emerges from the laboratory," *Photonic Spectra* **42**, 74+ (2008).
3. C. Monat, P. Domachuk, and B. J. Eggleton, "Integrated optofluidics: A new river of light," *Nat. Photonics* **1**, 106 – 114 (2007).
4. J. D. Joannopoulos, R. D. Meade, and J. N. Winn, *Photonic Crystals: Molding the Flow of Light* (Princeton University Press, Princeton, 1995).
5. K. Sakoda, *Optical Properties of Photonic Crystals* (Springer, 2001).
6. N. A. Mortensen and S. Xiao, "Slow-light enhancement of Beer-Lambert-Bouguer absorption," *Appl. Phys. Lett.* **90**, 141108 (2007).
7. N. A. Mortensen, S. Xiao, and J. Pedersen, "Liquid-infiltrated photonic crystals: enhanced light-matter interactions for lab-on-a-chip applications," *Microfluid. Nanofluid.* **4**, 117–127 (2008).
8. M. R. Lee and P. M. Fauchet, "Two-dimensional silicon photonic crystal based biosensing platform for protein detection," *Opt. Express* **15**, 4530–4535 (2007).
9. N. Skivesen, A. Têtù, M. Kristensen, J. Kjems, L. H. Frandsen, and P. I. Borel, "Photonic-crystal waveguide biosensor," *Opt. Express* **15**, 3169–3176 (2007).
10. S. Mandal and D. Erickson, "Nanoscale optofluidic sensor arrays," *Opt. Express* **16**, 1623–1631 (2008).
11. M. Lončar, A. Scherer, and Y. Qiu, "Photonic crystal laser sources for chemical detection," *Appl. Phys. Lett.* **82**, 4648 – 4650 (2003).
12. F. B. Arango, M. B. Christiansen, M. Gersborg-Hansen, and A. Kristensen, "Optofluidic tuning of photonic crystal band edge lasers," *Appl. Phys. Lett.* **91**, 223503 (2007).

13. M. Lu, S. Choi, C. J. Wagner, J. G. Eden, and B. T. Cunningham, "Label free biosensor incorporating a replica-molded, vertically emitting distributed feedback laser," *Appl. Phys. Lett.* **92**, 261502 (2008).
14. M. Lu, S. S. Choi, U. Irfan, and B. T. Cunningham, "Plastic distributed feedback laser biosensor," *Appl. Phys. Lett.* **93**, 111113 (2008).
15. J. Yang and L. Jay Guo, "Optical sensors based on active microcavities," *IEEE J. Sel. Top. Quantum Electron.* **12**, 143–147 (2006).
16. J. R. Masters, "HeLa cells 50 years on: the good, the bad and the ugly," *Nat. Rev. Cancer* **2**, 315–319 (2002).
17. ORMOCER is a registered trademark of Fraunhofer-Gesellschaft zur Förderung der angewandten Forschung e.V., Germany.
18. Micro resist technology GmbH, Berlin, Germany, www.microresist.de.
19. Pyrromethene 597, CAS Nr. 137829-79-9, acquired from Exciton Inc., www.exciton.com.
20. M. B. Christiansen, A. Kristensen, S. Xiao, and N. A. Mortensen, "Photonic integration in k-space: Enhancing the performance of photonic crystal dye lasers," *Appl. Phys. Lett.* **93**, 231101 (2008).
21. X. Cheng and L. J. Guo, "One-step lithography for various size patterns with a hybrid mask-mold," *Microelectron. Eng.* **71**, 288–293 (2004).
22. M. B. Christiansen, M. Schøler, and A. Kristensen, "Integration of active and passive polymer optics," *Opt. Express* **15**, 3931–3939 (2007).
23. Exiqon A/S, Vedbaek, Denmark, www.exiqon.dk.
24. M. H. Jakobsen and T. Koch, "Method of Photochemical Immobilization of Ligands using Quinones," US Patent Number 6033784 (2000).
25. T. Koch, N. Jacobsen, J. Fensholdt, U. Boas, M. Fenger, and M. H. Jakobsen, "Photochemical immobilization of anthraquinone conjugated oligonucleotides and PCR amplicons on solid surfaces," *Bioconjugate Chem.* **11**, 474–483 (2000).
26. E. S. Jauho, U. Boas, C. Wiuff, K. Wredstrom, B. Pedersen, L. O. Andresen, P. M. Heegaard, and M. H. Jakobsen, "New technology for regiospecific covalent coupling of polysaccharide antigens in ELISA for serological detection," *J. Immunol. Methods* **242**, 133–143 (2000).
27. G. Blagoi, S. Keller, F. Persson, A. Boisen, and M. H. Jakobsen, "Photochemical Modification and Patterning of SU-8 Using Anthraquinone Photolinkers," *Langmuir* **24**, 9929 – 9932 (2008).
28. N. Lue, G. Popescu, T. Ikeda, R. R. Dasari, K. Badizadegan, and M. S. Feld, "Live cell refractometry using microfluidic devices," *Opt. Lett.* **31**, 2759–2761 (2006).
29. R. Drezek, A. Dunn, and R. Richards-Kortum, "Light Scattering from Cells: Finite-Difference Time-Domain Simulations and Goniometric Measurements," *Appl. Opt.* **38**, 3651–3661 (1999).
30. N. Skivesen, R. Horvath, S. Thinggaard, N. B. Larsen, and H. C. Pedersen, "Deep-probe metal-clad waveguide biosensors," *Biosens. Bioelectron.* **22**, 1282 (2007).
31. B.-W. Chang, C.-H. Chen, S.-J. Ding, D. Chan-Hen Chen, and H.-C. Chang, "Impedimetric monitoring of cell attachment on interdigitated microelectrodes," *Sens. Actuators, B* **105**, 159 (2005).
32. S. Petronis, M. Stangegaard, C. B. V. Christensen, and M. Dufva, "Transparent polymeric cell culture chip with integrated temperature control and uniform media perfusion," *Biotechniques* **40**, 368–376 (2006).

1. Introduction

Optical label free biosensing has numerous applications in diverse fields such as healthcare, homeland security and environmental monitoring. A number of sensor principles exist [1], with different sensitivities and advantages. In order to find widespread use outside research labs, the sensors have to be compact, robust, and simple to use. To achieve this, sensors are commonly integrated with fluid handling systems and other functionalities in integrated optofluidic sensor systems [2, 3].

Sensing schemes based on photonic crystals (PhCs) [4, 5] are very well suited for integration, because they are compact and have tunable properties. Also, the sensitivity can be high because of dispersion effects [6] and because a substantial percentage of the optical energy can be in the evanescent fields [7].

A number of very sensitive PhC based biosensors made of high index dielectrics have been presented in the past few years, based on either PhC cavities [8] or waveguides [9]. The tunability of PhCs has been used to make multiplexed sensing, where several PhC sensors are addressed by the same bus waveguide [10]. One common complication in applying these sensors is that probe light must be coupled into μm sized waveguides on the chips.

One way to solve this problem and simplify use is to use PhC structures with optical gain,

enabling them to function as lasers. This was first demonstrated in high index semiconductor lasers [11], but the cost of such lasers remain relatively high and they are inherently difficult to integrate in polymer systems. Polymers remain the preferred material for integrated biosensors, because they are compatible with bioassays, transparent, cheap and can be structured very efficiently e.g. by injection molding. This keeps the device costs at a minimum, which is important because the chips are often single use. For single use polymer systems, organic dye doped polymer lasers are ideal as optofluidic evanescent wave sensor elements, because they are cheap to fabricate and very simple to use. Such lasers have been applied both for bulk refractive index sensing [12] and detection of monolayers of proteins [13, 14]. A further advantage of using active cavities is that their emission linewidths can be much narrower than the resonance peaks of their passive counterparts [15], which translates into a lower detection limit of the sensor.

PhC sensors are very suitable for detection of layers made of e.g. proteins, which have sizes far below the wavelength of light. However, for detection of larger objects, such as cells, scattering may become a problem, and if the PhC surface is covered in an irregular layer, the distributed effect of the PhC may break down.

Cells are often large enough to be distinguished in an optical microscope, and thus the most sensitive way to detect cell growth over time is to inspect the cells and count them. Conventional bright-field microscopy, which is usually utilized in the biomedical practice, is not sufficient in the high-throughput cell-based assays, however. The majority of standard cell viability tests and cytotoxicity assays exploit exogenous fluorophores or transfected fluorescent reporters. Although fluorescence-based methods allow for the easy determination of cell viability, the potential cytotoxicity and photobleaching of fluorophores should be taken into consideration. Thus, there is a significant need for a simple non-invasive detection method, which permits for real-time monitoring of cell growth.

In this paper we investigate the sensitivity of PhC band-edge lasers with a rectangular lattice to partial coverage with HeLa cells [16]. The lasers are chemically modified with a flexible UV activated anthraquinone based linker molecule, which enables selective binding of cells and molecules. When measuring in Phosphate Buffered Saline (PBS), which has a refractive index close to that of the cells, the emission wavelength depends linearly on the cell density on the sensor surface. This demonstrates that PhC lasers, which are cheap to fabricate and very simple to operate, can also be applied for sensing analytes substantially larger than the PhC lattice constant.

2. Design and fabrication

The lasers used were slab waveguides made of Ormocore, a type of ORMOCER [17] hybrid polymer, commercially available from micro resist technology GmbH [18]. They were doped with 5 μmol of the laser dye Pyrromethene 597 [19] per gram Ormocore. Figure 1 shows the laser layout with an inset atomic force microscope (AFM) image of the PhC imprinted into the surface. The lasers are pumped from above with 15 ns pulses from a compact frequency doubled Nd:YAG laser. The rectangular PhC provides feedback for in plane lasing, and also couples pump light into the chip plane, which increases the light output and lowers the laser threshold to a few hundred nJ/mm^2 . More information on the performance of the lasers and the optical measurement setup can be found in [20].

The lasers were fabricated by Combined Nanoimprint and Photolithography (CNP) [21]. CNP is a flexible wafer scale fabrication method, combining the resolution of nanoimprint lithography with the flexibility of UV lithography. More information on CNP and the fabrication parameters used to make the stamp can be found in [22]. The ORMOCER materials used here are very well suited for CNP fabrication of optical components. The refractive index can

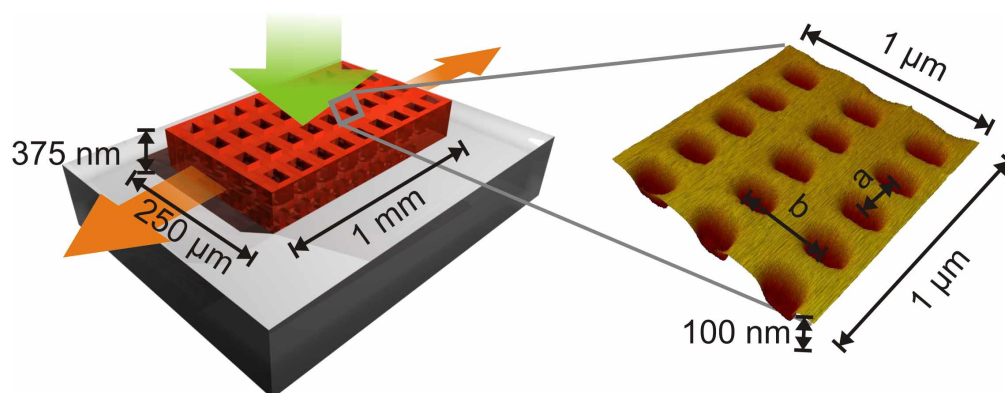


Fig. 1. Drawing showing a band-edge laser with an inset AFM image of the surface. The laser is made of Ormocore hybrid polymer doped with the laser dye Pyrromethene 597. It is fabricated on a glass substrate. The lasers are pumped optically from above, and emit in the chip plane. The rectangular PhC lattice increases pump absorption and provides laser feedback.

be tuned, and the fact that they are viscous fluids at room temperature makes it possible to perform the imprint without heating the stamp and substrate. This saves a substantial amount of processing time. The lasers were imprinted on a 10 cm diameter wafer in an EVG 520HE nanoimprinter at room temperature at a pressure of 10kN for 5 minutes. The stamp/substrate stack was UV flood exposed for 60 s in a 365 nm mask aligner at 7 mW/cm², before it was baked at a 90°C hotplate for 120 s. The reusable stamp was then separated from the substrate and the structures were developed in Ormodev, the commercially available ORMOCER developer, and rinsed in isopropyl alcohol.

3. Photochemical modification

Chemical modification of the lasers was done with UV activated linker molecules (AQ-Link) commercially available from Exiqon A/S[23]. The technology has previously been used to introduce various functional groups and biomolecules onto a variety of polymers[23, 24], including DNA[25] and polysaccharide antigens derived from Gram-negative bacteria[26]. Recently, the method has been extended to create chemical patterns on the photoresist SU-8 with a resolution limit of app. 1 μm[27]. AQ-Link molecules are available from Exiqon A/S with a number of different functional groups. In this work, electrophilic (AQ-E) and primary amine (AQ-NH₂) end groups have been used.

The lasers were modified in a petri dish with 10 ml milliQ water with either 2 μg/ml AQ-E or a 100 μM concentration of AQ-NH₂. Irradiation was done in a photoreactor with a relatively broad spectrum centered around 365 nm at approximately 14 mW/cm² for 45 minutes. After UV treatment the samples were washed in MilliQ water to remove excess reagent (3x5 min) and dried at 37°C for 30 minutes.

4. Verification of surface modification

After AQ-E attachment and rinse 0.5 μl of biotin-amine solution was spotted on each laser. The solution was a 100 mM carbonate buffer (pH 9.6) with biotin-amine. The biotin-amine concentrations used were 250.0 μg/ml, 125.0 μg/ml, 62.5 μg/ml, 31.3 μg/ml, and 15.6 μg/ml. The chips were left to incubate in a humidity chamber over a saturated NaCl solution over night and washed (3x5 min.) in a 100 mM phosphate buffered saline containing 0.5 % Tween

20 (PBS-T).

All chips were then incubated in centrifugation tubes in PBS-T buffer with 1.5 $\mu\text{g/ml}$ streptavidin. A third of the streptavidin molecules had Cy5 markers. After incubating over night the chips were washed 3x5 min. in PBS-T and 3x5 min. in milliQ water and dried.

In order to quantify the fluorescence signal from the laser chips they were taped on a microscopy slide and scanned in a microarray scanner (Packard Biochip Technologies). The scanner was fitted with a 532 nm green laser and a 650 nm red laser. Both were used, since the PM597 dye fluoresces under excitation with the green laser, making it possible to see the lasers, and the Cy5 dye on the streptavidin fluoresces under excitation with the red laser.

Figure 2 shows the resulting scanner images. As seen in the panels (a), (c), and (e), the lasers are visible under green excitation light, because of the PM597 laser dye. It is also clear from panel (b) that the amount of bound streptavidin depends on the concentration of the spotted biotin-amine. The untreated device shows no fluorescence under red excitation, as seen in panel (f). Panel (d) shows the device spotted with the 62.5 $\mu\text{g/ml}$ biotin-amine solution under red excitation. The laser itself lights up brighter than the surrounding area, which is expected since the AQ molecules should not bind to glass. The blue circular area shows where the spot has been positioned, however. This signal is attributed to organic residues from the fabrication process that has been modified by the AQ-E molecules.

5. Cell culture

AQ-NH₂ was used to make a positively charged surface for attaching HeLa cervical carcinoma cells [16] to the lasers. Working with cells requires the lasers to be sterile, so after AQ-Link attachment the lasers were cleaned for 30 minutes in 70% ethanol, three times in 10 mM sterile phosphate buffered saline (PBS), and three times in sterile-filtred water (Sigma-Aldrich). They were then placed in the growth container, in this case a 24 well cell growth plate, and covered in a volume of cell growth medium (1 ml).

HeLa cells are quite large, typically 10 to 20 μm , and as such are not particularly difficult to see in a microscope. They are used here because their refractive index of 1.38 at 632 nm [28] is typical for mammalian cells. HeLa cells were cultured in DMEM medium (Invitrogen) supplemented with 10% fetal bovine serum - FBS (Sigma-Aldrich), 2 mM L-glutamine (Sigma-Aldrich), 100 U/ml penicillin (Sigma-Aldrich), 100 $\mu\text{g/ml}$ streptomycin (Sigma-Aldrich) and grown until confluency at 37°C in a humidified atmosphere containing 95% air and 5% CO₂. Cells were harvested at 80-90% confluence by trypsinization (0.05% trypsin-EDTA), washed, and resuspended in cell growth medium. Cell counting was performed using a hemocytometer. Different initial concentrations of cells were prepared and seeded into each test well of a 24-well plate. Each test well contained a laser. The cell densities on the lasers were determined after 24 hours of cell seeding. Then the cell growth medium was removed, the cells were washed with sterile PBS and left on the lasers in PBS buffer. HeLa cells in PBS buffer do not preserve the typical morphology due to the absence of the ions determining the elongated shape of cells.

Figure 3 shows microscope images of cell treated lasers, dried by leaving them in air for approximately 12 hours. The devices in panels (a), (b) and (c) are all treated with AQ-NH₂ and decreasing number of cells. It is clear how the coverage depends on the number of cells in the well during growth. Panel (d) is a device subjected to the same cell number and growth conditions as the device in panel (a), but without the AQ-NH₂. Cell growth was not observed on any devices without AQ-Link treatment.

6. Results and discussion

Optical characterization was performed by measuring the emission wavelength of the lasers in PBS buffer ($n = 1.33$ [29]) before and after the cell treatment. The results are presented

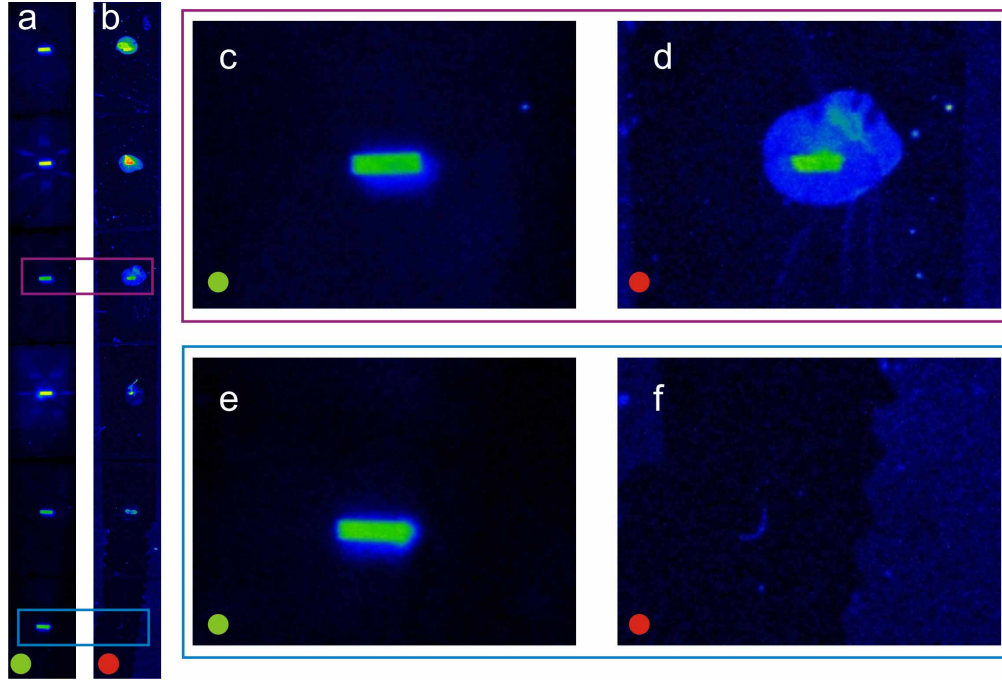


Fig. 2. Fluorescence signals from the lasers treated with AQ-Link, biotine-amine, and Cy5 marked streptavidin. The excitation color is indicated in the bottom left of each image. **(a)** Signal from all lasers under green excitation. The five upper lasers were treated with biotin concentrations decreasing from the top. The last device was untreated. All lasers are visible because the PM597 dye is fluorescing. **(b)** Same as **(a)**, but with red excitation. It is clear how the Cy5-Streptavidin signal decrease with the spotted biotin concentration. **(c)** and **(d)** Closer images of third device (62.5 $\mu\text{g/ml}$ of biotin-amine) excited with green and red light, respectively. Note that the biotin spot is visible, but the Cy5 signal is stronger on the laser itself. **(e)** and **(f)** Closer images of the untreated device, again excited with green and red, respectively. The PM597 signal is visible, while no Cy5 streptavidin signal is present, as expected.

in Table 1 and Fig. 4. 500 cells per mm^2 corresponds to a close packed film of cells in the growth medium. Measurements were done in PBS, to avoid absorption of pump light in the cell medium, which was dyed with Phenol red to monitor the pH value.

The ethanol cleaning prior to cell growth caused a blue-shift of the lasers of 0.76 nm, hence the negative off-set on the data. In Fig. 4 this offset has been removed from the data. A linear relation between cell coverage and wavelength is seen, with a slope of $1.25 \times 10^{-3} \text{ nm} \cdot \text{mm}^2$.

Assume the laser is emitting at a wavelength λ when covered with a fluid of index n . The laser is then partially covered in cells with a refractive index of $n + \Delta n$, causing the wavelength to shift $\Delta\lambda$. From first-order perturbation theory we in general have

$$\frac{\Delta\lambda}{\Delta n} = \frac{\lambda}{n} f_c, \quad (1)$$

where f_c is the fraction of the mode optical energy in the cells. We assume that a cell has a volume V and covers an area of A and that V/A exceeds the decay length of the evanescent optical field of the laser mode. If $\sqrt{A} \gg a$, the lattice constant of the PhC, the average field overlap with the cell will not depend on the particular position of the cell. In that case, we get

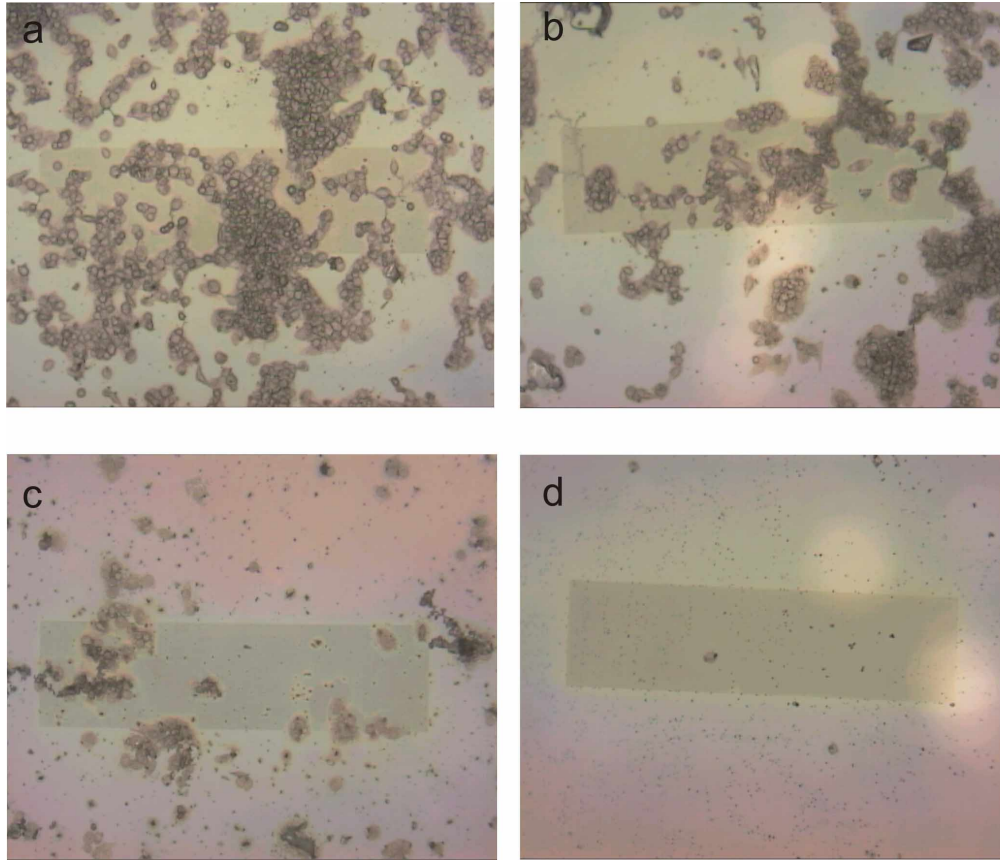


Fig. 3. Laser devices after HeLa cell attachment procedure and drying in air. **(a)** Laser treated with AQ-NH₂ and 2×10^5 cells in suspension. **(b)** Laser treated with AQ-NH₂ and 5×10^4 cells in suspension. **(c)** Laser treated with AQ-NH₂ and 1×10^4 cells in suspension. **(d)** Laser treated with 2×10^5 cells in suspension, but no AQ-NH₂.

Table 1. Cell density and wavelength shift for lasers. The wavelength change is measured in PBS before and after cell growth.

Chip number	Cell density mm^{-2}	Wavelength change nm
1	0	-0.65 ± 0.2
2	150	-0.71 ± 0.2
3	260	-0.44 ± 0.2
4	500	-0.08 ± 0.2

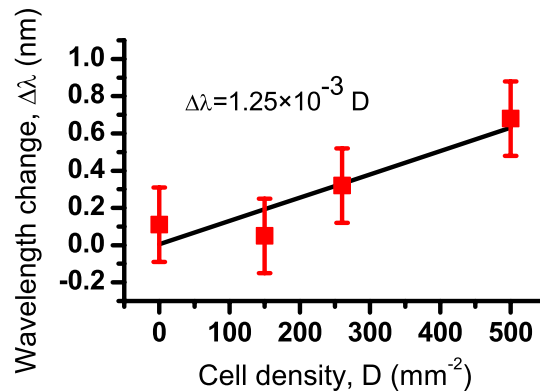


Fig. 4. Measured data and linear fit for the wavelength change in PMS as a function of cell surface density. 500 cells per mm 2 corresponds to a dense film in growth medium, but in PBS the cells contract. Note that the data has been normalized to intercept the origin.

$f_c = fC$, where f is the energy fraction in the upper evanescent field and C is the fractional coverage of cells, satisfying $0 < C < 1$. For a 375 nm thick Ormocore waveguide $f = 4.9\%$, and the emission wavelength of the lasers in PBS is around 602 nm. Inserting these numbers yields an expected wavelength shift of 1.1 nm for complete cell coverage. The measured shift for complete coverage is thus a little more than half the calculated shift. This difference can be attributed to the fact that the elongated cells contract when the growth medium is replaced with PBS, and thus C will be below 1, as seen in Fig. 3(a). In principle the experiment could also be performed in growth medium, if no pH indicator is added.

The linear dependence of emission wavelength on cell coverage shows that the entire optical mode of the PhC laser is influenced by the cells, although the cells are much larger than the PhC lattice constant, and the coverage is very irregular. However, the fact that cell covered lasers do not work when dried, is an indication that this is only occurring when the cells perturb the mode to a small extent. If the index difference becomes too large the distributed feedback of the laser simply breaks down. Also, it is important to note that f is quite small for these lasers. This also limits the extent to which the mode can be influenced. It also limits the sensitivity, however, so a trade-off must be made when designing lasers for sensing larger objects. This is in contrast to the requirements for measuring sub-wavelength objects or bulk refractive index, where f , and thus the sensitivity is normally maximized[7].

The measured sensitivity, from the slope of the fit in Fig. 4, is 1.25×10^{-3} nm \cdot mm 2 , corresponding to approximately 5×10^{-3} nm per cell sitting on the laser, which has a size of 0.25 mm 2 . It should be possible to shrink the lasers to a tenth of the current size. In that case, a cell would tune the lasers 5×10^{-2} nm, which means that a few cells can be detected, depending on the quality of the measurement setup used.

This detection limit is comparable to e.g. metal clad waveguide waveguide cell sensors [30], but the strength of this approach is the cheap parallel fabrication and the very simple operation, where a pump laser simply needs to illuminate the dye laser to operate it.

A common competing non-optical method is electrochemical sensing, which essentially give the same information as the PhC band edge lasers investigated here, and also with the ability to detect a few cells[31]. Electrode sensors however have a number of drawbacks such as 1) electrodes has to be incorporated into the chip, 2) electrodes provides heterogeneous cell culture surface, 3) difficulties to scale the number of electrode sensors, 4) a short life expectancy of the sensor. The PhC band edge lasers presented here can be integrated densely in all-polymer

optofluidic sensor chips and the dye will last for years if the sensor is interrogated e.g. every ten minutes.

Modifying the lasers with AQ-Link molecules is quite simple and very flexible, because AQ-Link molecules exist with several different end groups. Since the molecule is UV activated, it is possible to modify lasers selectively by exposing through a mask, very similar to UV lithography. This makes it possible to make several sensors selective to different analytes on one chip.

In a sensor setup an unmodified reference laser would typically be placed close to the sensing laser, to eliminate problems with e.g. temperature fluctuations. This also means that the negative tuning of the lasers caused by cleaning in ethanol does not necessarily constitute a severe problem. However, the phenomenon may be an indication that the Ormocore is not cross-linked fully. Better cross-linking could be achieved by UV exposing and/or baking the lasers after development.

7. Conclusion

Our results, where the wavelength of photonic crystal band edge lasers is shown to depend linearly on coverage with HeLa cells, demonstrate that photonic crystal based label free biosensors can also be used to detect analytes far larger than the lattice constant. However, it must be ensured that the optical mode is only perturbed to a small extent, in order to avoid breakdown of the distributed effect of the photonic crystal.

The lasers presented here are fabricated in a parallel wafer scale process and chemically modified with a flexible UV activated linker molecule. This, combined with very simple operation, make the lasers candidates for implementation in cheap integrated optofluidic sensor systems, which could also allow for real time monitoring of cell growth[32].